

## Validating (d, $\gamma$ ) as a Surrogate for Neutron Capture

A. Ratkiewicz<sup>1,a</sup>, J.A. Cizewski<sup>1</sup>, S.D. Pain<sup>2</sup>, A.S. Adekola<sup>1</sup>, J.T. Burke<sup>3</sup>, R.J. Casperson<sup>3</sup>, N. Fotiadis<sup>4</sup>, M. McCleskey<sup>5</sup>, S. Burcher<sup>1</sup>, C.M. Shand<sup>1,6</sup>, R.A.E. Austin<sup>7</sup>, T. Baugher<sup>1</sup>, M.P. Carpenter<sup>8</sup>, M. Devlin<sup>4</sup>, J.E. Escher<sup>3</sup>, S. Hardy<sup>1,6</sup>, R. Hatarik<sup>3</sup>, M.E. Howard<sup>1</sup>, R.O. Hughes<sup>9</sup>, K.L. Jones<sup>10</sup>, R.L. Kozub<sup>11</sup>, C.J. Lister<sup>12</sup>, B. Manning<sup>1</sup>, J.M. O'Donnell<sup>4</sup>, W.A. Peters<sup>13</sup>, T.J. Ross<sup>9</sup>, N.D. Scielzo<sup>3</sup>, D. Seweryniak<sup>8</sup>, and S. Zhu<sup>8</sup>

<sup>1</sup>Department of Physics and Astronomy, Rutgers University, New Brunswick, NJ 08903, USA

<sup>2</sup>Physics Division, Oak Ridge National Laboratory, Oak Ridge, TN 37831, USA

<sup>3</sup>Lawrence Livermore National Laboratory, Livermore, CA 94550, USA

<sup>4</sup>Los Alamos National Laboratory, Los Alamos, NM 87545, USA

<sup>5</sup>Cyclotron Institute, Texas A&M University, College Station, TX 77843, USA

<sup>6</sup>Department of Physics, University of Surrey, Guildford, Surrey, GU2 7XH, UK

<sup>7</sup>Astronomy and Physics Department, Saint Mary's University, Halifax, NS BH3 3C3, Canada

<sup>8</sup>Physics Division, Argonne National Laboratory, Argonne, IL 60439, USA

<sup>9</sup>Department of Physics, University of Richmond, VA 23173, USA

<sup>10</sup>Department of Physics and Astronomy, University of Tennessee, Knoxville, TN 37996, USA

<sup>11</sup>Physics Department, Tennessee Technological University, Cookeville, TN 38505, USA

<sup>12</sup>Department of Physics and Applied Physics, University of Massachusetts Lowell, Lowell, MA 01854, USA

<sup>13</sup>Oak Ridge Associated Universities, Oak Ridge, Tennessee 37831, USA

**Abstract.** The  $r$ -process is responsible for creating roughly half of the elements heavier than iron. It has recently become understood that the rates at which neutron capture reactions proceed at late times in the  $r$ -process may dramatically affect the final abundance pattern. However, direct measurements of neutron capture reaction rates on exotic nuclei are exceptionally difficult, necessitating the development of indirect approaches such as the surrogate technique. The (d, $\gamma$ ) reaction at low energies was identified as a promising surrogate for the (n, $\gamma$ ) reaction, as both reactions share many characteristics. We report on a program to validate (d, $\gamma$ ) as a surrogate for (n, $\gamma$ ) using <sup>95</sup>Mo as a target. The experimental campaign includes direct measurements of the  $\gamma$ -ray intensities from the decay of excited states populated in the <sup>95</sup>Mo(n, $\gamma$ ) and <sup>95</sup>Mo(d, $\gamma$ ) reactions.

### 1 Introduction

Neutron capture reactions on unstable nuclei are of broad interest due to their importance to interpretations of  $r$ -process abundance patterns [1] and applications to nuclear security and nuclear energy. However, direct measurements of such reactions in the neutron-rich areas of interest are very difficult or impossible to carry out due to the unstable nature of both neutrons and the targets. Therefore, techniques to indirectly extract these cross sections must be developed. When the nuclear reaction in question ( $a + A \rightarrow B^* \rightarrow c + C$ ) forms a compound nucleus ( $B^*$ ), a system sufficiently long-lived for its excitation energy to be evenly distributed over all of the nucleons comprising it, the entrance channel is “forgotten” and the decay of the compound nucleus ( $c + C$ ) is independent of the entrance channel. The cross section for this reaction can be expressed in the Hauser-Feshbach formalism as [2]:

$$\sigma_{\alpha\chi}(E_n) = \sum_{J,\pi} \sigma_{\alpha}^{CN}(E_{ex}, J, \pi) G_{\chi}^{CN}(E_{ex}, J, \pi). \quad (1)$$

<sup>a</sup>e-mail: a.ratkiewicz@rutgers.edu

Here,  $\alpha$  denotes the entrance channel,  $\sigma_{\alpha}^{CN}(E_{ex}, J, \pi)$  the formation cross section for the compound nucleus, and  $G_{\chi}^{CN}(E_{ex}, J, \pi)$  represents the decay of the compound nucleus through the exit channel  $\chi$ . In practice, the formation cross sections can be reliably calculated with optical potentials, but the branching ratios are difficult to determine with sufficient accuracy to constrain neutron capture cross sections. It is thus necessary to constrain  $G_{\chi}^{CN}$  through experiment.

The same compound nucleus may be formed through a “surrogate reaction”, ( $d + D \rightarrow B^* + b$ ), in which the projectile-target system are more amenable to experimental study and the decay of the compound nucleus ( $B^*$ ) is observed in coincidence with a particle represented by  $b$ . Then the probability for forming the compound nucleus created through the entrance channel  $\delta$  and decaying through the exit channel  $\chi$  can be expressed as [2]:

$$P_{\delta\chi}(E_{ex}) = \sum_{J,\pi} F_{\delta}^{CN}(E_{ex}, J, \pi) G_{\chi}^{CN}(E_{ex}, J, \pi), \quad (2)$$

where  $F_{\delta}^{CN}(E_{ex}, J, \pi)$  represents the probability of forming the compound nucleus  $B^*$  with an excitation energy

of  $E_{ex}$ . The Weisskopf-Ewing (WE) approximation [3] is often employed in order to make the calculation of the branching ratio tractable. This approximation makes the assumption that the branching ratios depend only on the energy, not the spin or parity, of the excited state and the branching ratio simplifies:  $G_{\chi}^{CN}(E_{ex}, J, \pi) \rightarrow \mathcal{G}_{\chi}^{CN}(E_{ex})$ . If the surrogate and desired reactions form the “same” compound nucleus, the probability of forming the compound nucleus is:  $\sum_{J,\pi} F_{\delta}^{CN}(E_{ex}, J, \pi) = 1$ . Therefore Eq. 2 becomes:

$$P_{\delta\chi}(E_{ex}) = \mathcal{G}_{\chi}^{CN}(E_{ex}). \quad (3)$$

The branching ratio can then be determined experimentally by measuring the number of surrogate events ( $N_{\delta}$ ) and the number of coincidences between the observable tagging the relevant exit channel of the reaction and the compound nucleus ( $N_{\delta\chi}$ ), corrected by the efficiency of the detector system for the detection of that observable ( $\epsilon_{\chi}$ ) [2]:

$$P_{\delta\chi}(E_{ex}) = \frac{N_{\delta\chi}}{N_{\delta}\epsilon_{\chi}}. \quad (4)$$

The cross section for the desired reaction can be determined from Eq. 1:

$$\sigma_{\alpha\chi}^{CN}(E_{ex}) = \sigma_{\alpha}^{CN}(E_{ex}) P_{\delta\chi}(E_{ex}). \quad (5)$$

Theoretical models suggest that it may be appropriate to employ the Weisskopf-Ewing approximation for neutron energies above about 3 MeV [4]. However, the  $(n,\gamma)$  cross section is enhanced at lower energies, and several studies [4–7] have shown that the WE approximation cannot be used to extract neutron capture cross sections in the energy range appropriate for  $(n,\gamma)$  reactions with large cross sections when  $E_n < 1$  MeV. However, Escher *et al.* [6] have suggested that a “serendipitous” approach may be valid when the spin-parity of the surrogate reaction is similar to that of neutron capture. Indeed, Hatarik *et al.* [5] have shown that by focusing on the side-feeding of low-lying transitions in the  $(d, p\gamma)$  surrogate reaction the ratios of the  $(n,\gamma)$  cross sections can be reproduced.

## 2 Surrogate Measurements in Normal Kinematics

### 2.1 Experimental Setup

The work of Forssén *et al.* [4] emphasizes the need for a benchmarking of the surrogate reaction method, in which known  $(n,\gamma)$  cross sections are compared to cross sections extracted from a surrogate experiment. The  $(d, p\gamma)$  reaction is a natural candidate for an  $(n,\gamma)$  surrogate – like  $(n,\gamma)$  reactions, low-energy  $(d, p\gamma)$  reactions primarily involve the transfer of a nucleon with low angular momentum. The choice of the target was informed by benchmarking requirements – first that the neutron capture cross section should be known up to at least 200 keV. Second, the analysis is simplified if the daughter nucleus is an even-even one in which a strong  $2_1^+ \rightarrow 0_{g.s.}^+$  transition collects much of the decay strength from the decay of the compound nucleus. As the formation and decay of the compound nucleus must be modeled and these models are sensitive to

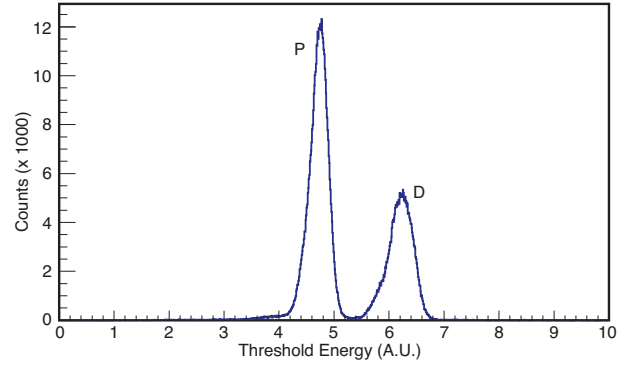


**Figure 1.** Particle identification histogram constructed through the linearization of energies (Eq. 6) deposited in forward-angle  $\Delta E$  and  $E$  detectors by particles from the reaction of a 12.5 MeV deuteron beam on a  $^{95}\text{Mo}$  target. The linearization technique allows clear discrimination between the peaks due to protons (lower energy, labeled “P”) and deuterons (higher energy, labeled “D”). Approximately one hour of data are shown. Elastically scattered deuterons are suppressed by applying a cut on larger angles.

the structure of the nucleus, so the structure of the nucleus chosen for the benchmarking experiments should be well known.  $^{95}\text{Mo}$  meets all of these requirements, with the  $(n,\gamma)$  cross section having been directly measured by Musgrove *et al.* [8].

The  $^{95}\text{Mo}(d, p\gamma)$  reaction was measured with the **Silicon Telescope Array for Reactions with Livermore and Texas A&M University and Richmond (STARLiTeR)** detector system currently located at the Texas A&M Cyclotron Institute [9, 10]. Light ejectiles were detected in two silicon telescopes 1.6 cm upstream and 2.1 cm downstream of the target respectively. Each telescope was composed of a detector for measuring energy loss ( $\Delta E$ , 140  $\mu\text{m}$  thick) and total energy ( $E$ , 1000  $\mu\text{m}$  thick). Each detector was segmented into 48 rings on the front side, bussed together in pairs, and 16 sectors on the back side, also bussed together in pairs. A 16  $\mu\text{m}$  thick aluminum shield was used to protect the forward angle detector from  $\delta$  electrons. Four high-purity germanium clover detectors inside of BGO Compton-suppressing shields were located at 90, 220, 270, and 320 degrees with respect to the beam axis in the laboratory frame.

A 12.5-MeV beam of deuterons was provided by the K150 cyclotron at the Cyclotron Institute at Texas A&M University, and impinged on a 0.96  $\text{mg}/\text{cm}^2$  thick molybdenum target foil enriched to 96.8% in  $^{95}\text{Mo}$ . The primary contaminant was  $^{96}\text{Mo}$  with an abundance of 1.54% [11]. The data acquisition trigger condition required that an above-threshold signal (about 400 keV) be detected in both detectors in either the forward or backward telescope. When this condition was satisfied, any  $\gamma$  rays detected in coincidence with the triggering event in the telescopes were recorded.

Particle identification was accomplished by the range-energy method discussed in Ref. [12]. Protons and deuterons were discriminated through applying the follow-

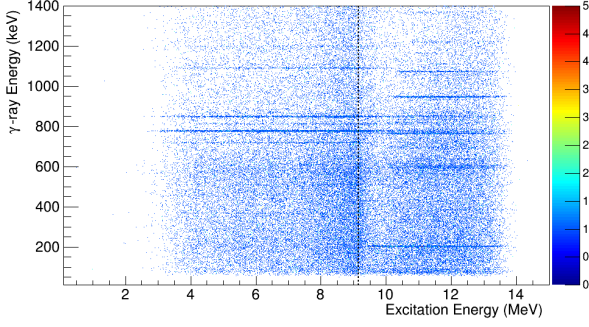


**Figure 2.** (color online) Matrix showing coincidences between the reconstructed center of mass  $^{96}\text{Mo}$  excitation energies of protons (MeV) detected in the forward telescope and  $\gamma$  rays (keV) detected in the four HPGe clovers. The neutron separation energy ( $S_n = 9.152$  MeV) is indicated by the dashed line. Approximately one hour of data are shown.

ing equation:

$$R = (E_1 + \Delta E_1)^\alpha - E_1^\alpha \quad (6)$$

where  $\alpha = 1.68$  is a constant related to the stopping power of silicon. The particle identification histogram is shown in Fig. 1.

The silicon detectors were calibrated using a  $^{226}\text{Ra}$   $\alpha$  source. Following the calibration, the nuclear excitation energy ( $E_{ex}$ ) was calculated from  $E_{ex} = E_{beam} - E_{proton} - E_{recoil}$ , where  $E_{beam} = 12.5$  MeV is the beam energy, and  $E_{proton}$  (the proton energy) and  $E_{recoil}$  (the energy of the recoiling  $^{95}\text{Mo}$  target nucleus) were reconstructed on an event-by-event basis. A matrix showing the proton-gated coincidences between events in the reconstructed excitation energy spectrum and  $\gamma$  rays detected in the clover detectors is shown in Fig. 2. The  $^{95}\text{Mo}(d,p\gamma)$  reaction can populate states below the neutron separation energy of  $^{96}\text{Mo}$  ( $S_n = 9.152$  MeV [13]), as well as above  $S_n$ , which corresponds to the  $(n, \gamma)$  surrogate, characterized by  $\gamma$ -ray de-excitations to the ground state of  $^{96}\text{Mo}$ . States populated significantly above the neutron separation energy in  $^{96}\text{Mo}$  can also decay to the ground state in  $^{95}\text{Mo}$ , acting as the  $(n, n'\gamma)$  surrogate. The transition between the  $(n, \gamma)$  and  $(n, n'\gamma)$  decay channels can be clearly seen in Fig. 2.

## 2.2 Preliminary Results

The probability that the final nucleus with excitation energy  $E_{ex}$  in the  $^{95}\text{Mo}(d,p\gamma)$  reaction de-excites through  $\gamma$ -ray emission ( $P_{p\gamma}$ ) was determined following the method used by Scielzo *et al.* in [7, 14]:

$$P_{p\gamma}(E_{ex}) = \frac{(1 - \alpha_{IC}) N_{p\gamma}(E_{ex})}{\epsilon_\gamma f(E_{ex}) N_p(E_{ex})}, \quad (7)$$

where  $\alpha_{IC}$  is the internal conversion coefficient for the transition,  $f(E_{ex})$  is the fraction of the  $\gamma$ -ray cascades which de-excites through the transition in question,  $\epsilon_\gamma$  is the  $\gamma$ -ray detection efficiency,  $N_{p\gamma}$  is the number of coincidences between a proton and a  $\gamma$ -ray characteristic of

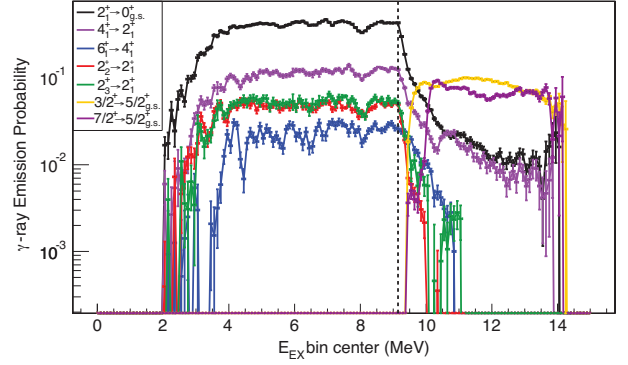


**Figure 3.** (color online) Emission probabilities calculated from the intensities of transitions in  $^{96}\text{Mo}$  (the  $(n, \gamma)$  surrogate) and  $^{95}\text{Mo}$  (the  $(n, n')$  surrogate) are displayed. The dashed line corresponds to the neutron separation energy in  $^{96}\text{Mo}$ ,  $S_n = 9.152$  MeV [13]. The probability of emission of  $\gamma$  rays from *yrast* transitions in  $^{96}\text{Mo}$  are indicated by the black ( $2_1^+ \rightarrow 0_{g.s.}^+$ ), pink ( $4_1^+ \rightarrow 2_1^+$ ), and blue ( $6_1^+ \rightarrow 4_1^+$ ) lines. Emission probabilities for non-*yrast* transitions in  $^{96}\text{Mo}$  are shown in red ( $2_2^+ \rightarrow 2_1^+$ ) and green ( $2_3^+ \rightarrow 2_1^+$ ). Emission probabilities for transitions created through the decay of states above the  $(n, n')$  surrogate threshold are shown in yellow ( $3/2^+ \rightarrow 5/2_{g.s.}^+$ ) and purple ( $7/2^+ \rightarrow 5/2_{g.s.}^+$ ).

the transition of interest, and  $N_p$  is the number of proton singles detected. For the case of  $^{96}\text{Mo}$ , in which very few transitions are strongly internally converted, Eq. 7 becomes:

$$P_{p\gamma}(E_{ex}) \approx \frac{1}{\epsilon_\gamma} \frac{N_{p\gamma}(E_{ex})}{N_p(E_{ex})}. \quad (8)$$

The particle- $\gamma$  excitation matrix shown in Fig. 2 was projected onto the ordinate in 100-keV increments. The resulting spectra of low-lying  $\gamma$  rays emitted in the decay of excited states as a function of excitation energy in  $^{95,96}\text{Mo}$  were fit using the ROOFIT package [15]. The resulting intensities are shown in Fig. 3.

The  $^{96}\text{Mo}$  *yrast* transitions are the strongest observed, with the  $2_1^+ \rightarrow 0_{g.s.}^+$  transition (at 778 keV) the strongest, the  $6_1^+ \rightarrow 4_1^+$  transition (at 812 keV) being the weakest of these, and no evidence of a  $8_1^+ \rightarrow 6_1^+$  transition (at 538 keV [13]). As Fig. 3 shows, the emission probability for the  $2_1^+ \rightarrow 0_{g.s.}^+$  transition below  $S_n$  is nearly 1, supporting the conclusion that this transition collects almost all of the  $\gamma$ -ray intensity. Current analysis is focused on expanding the analysis to the full spectrum of  $\gamma$  rays produced in the de-excitation of  $^{96}\text{Mo}$ , including those that directly populate the ground state, to extract the full emission probability (Eq. 8).

Future work will include exploiting the  $2_1^+ \rightarrow 0_{g.s.}^+$  as a collecting transition and the side-feeding of low-lying levels to calculate  $(n, \gamma)$  surrogate cross sections that would be compared to direct measurements of the  $(n, \gamma)$  cross section by Musgrove *et al.* in [8].

## 2.3 Comparison to $(n, \gamma)$ Measurements

As displayed in Fig. 3, many surrogate reaction studies focus on the intensity of the strongest, often *yrast*, transi-

tions as a function of excitation energy or effective neutron energy. The  $^{95}\text{Mo}(n, \gamma)$  reaction was measured at the Los Alamos Neutron Science Center (LANSCE) to provide analogous information on the intensity of  $\gamma$ -ray transitions as a function of neutron energy. Two measurements were made. The first exploited a small array of HPGe detectors on flight-path 12 at the Lujan Center, enabling measurements from  $20 \text{ eV} < E_n < 200 \text{ keV}$ . The same  $^{96}\text{Mo}$  transitions were observed in these data as those summarized in Fig. 3, including the  $6^+ \rightarrow 4^+$  812-keV transition at the higher neutron energies, and no evidence for the  $8^+ \rightarrow 6^+$  transition. The second measurement at  $E_n > 200 \text{ keV}$  was made at WNR with the GEANIE array of Compton-suppressed HPGe detectors [16]. Preliminary results show the  $(n, n')$  channel dominating above the 204-keV threshold for populating the first excited state in  $^{95}\text{Mo}$ . The goal is to use the intensities of the transitions as a function of neutron energy measured in actual  $(n, \gamma)$  reactions to extract a neutron capture cross section using the same techniques as are deployed in a surrogate measurement and compared to the results from direct  $^{95}\text{Mo}(n, \gamma)$  cross section measurements [8].

### 3 Surrogate Reactions in Inverse Kinematics

The STARLiTeR detector is optimized to measure transfer reactions in normal kinematics, which limits possible targets to those isotopes which are stable or very long-lived. Measuring surrogate reactions in neutron-rich regions of the nuclear chart of interest to astrophysical, nuclear security, and nuclear energy applications requires a detector suited for inverse kinematics measurements with radioactive ion beams and capable of measuring light particles and  $\gamma$  rays in coincidence. Such a particle- $\gamma$  spectrometer must have high  $\gamma$ -ray detection efficiency (as the rates of available beams are likely to be low) and high energy resolution for  $\gamma$ -ray and particle detection, as some exotic nuclei have dense excited state structure. Only HPGe detectors which cover a large fraction of the solid angle around the target are currently able to satisfy the simultaneous requirements of high  $\gamma$ -ray energy resolution and detection efficiency. The Gammasphere array of 110 Compton-suppressed HPGe detectors [17] combines high geometric efficiency with target area large enough to support the mounting of the light charged-particle detector ORRUBA [18]. ORRUBA (the Oak Ridge RUTgers Barrel Array) is a modestly-segmented silicon detector array which combines high angular resolution ( $\Delta\theta = 1$  degree) with high energy resolution ( $\sim 28 \text{ keV}$  FWHM for a 5.8 MeV  $\alpha$ -particle). The ORRUBA barrel is composed of rectangular position sensitive 1 mm-thick detectors to measure total energy ( $E$ ) which are segmented into four resistive strips on the front and four blocks on the back. A telescope can be made by combining the  $E$  detectors with  $65 \mu\text{m}$ -thick non-resistive  $\Delta E$  detectors which are segmented into eight strips on the front. ORRUBA can be augmented with annular endcap detectors, each covering  $\sim 90^\circ$  of the polar angle, which are segmented into 32 variably-pitched strips

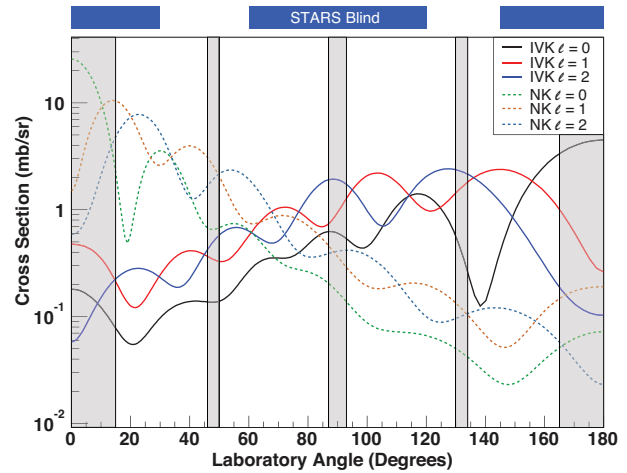


**Figure 4.** (color online) DWBA calculation of the differential cross section for different  $\ell$ -transfers to a 1-MeV excited state in  $^{96}\text{Mo}$  from the  $^{95}\text{Mo}(d,p)$  reaction at an energy of 10 MeV-A for normal (dashed lines, “NK”) and inverse (solid lines, “IVK”) kinematics. The areas shaded in grey are the angles to which GODDESS is blind. The angles to which STARS is blind are indicated by the blue boxes at the top of the figure.

on the front side and four sectors on the back side. Up to three layers of these endcap detectors can be configured into a telescope, with the  $\Delta E$  layer 100- $\mu\text{m}$  thick and the  $E$  layer 1-mm thick. The entire array covers 75% of the polar angle between 15 and 165 degrees in the laboratory frame. Figure 4 shows the relative angular coverage for ORRUBA and STARLiTeR. Together, the Gammasphere and ORRUBA systems form **Gammasphere-ORRUBA: Dual Detectors for Experimental Structure Studies (GODDESS)** [19, 20]. When it is necessary to detect the heavy recoiling particles, GODDESS can be supplemented by the Fragment Mass Analyzer (FMA) [21] or (when the beam is too rigid to be bent by the FMA) a re-entrant high-rate ionization chamber of a design similar to the one described by Chae *et al.* in [22].

The high geometric efficiency provided by GODDESS will allow surrogate reactions to be measured in inverse kinematics with radioactive beams, opening exotic, neutron-rich areas of the nuclear chart for exploration with this technique. Additionally, by covering a large fraction of the solid angle, GODDESS enables the simultaneous measurement of pickup and stripping reactions – the  $(n, \gamma)$  surrogate can be measured “for free” in any measurement of a stripping reaction. The GODDESS detector system is nearly complete, with first beam expected late 2014 or early 2015. One of the first planned experiments with GODDESS is a measurement of the  $^{95}\text{Mo}(d, p\gamma)$  reaction in inverse kinematics. This measurement will extend to inverse kinematics the validation of the  $(d, p\gamma)$  reaction as a surrogate for the  $(n, \gamma)$  reaction.

### 4 Summary

The  $(d, p\gamma)$  reaction is a promising surrogate for the neutron capture reaction, in particular on nuclei away from

stability important for understanding  $r$ -process nucleosynthesis and applications for nuclear security and energy. Preliminary results from the normal kinematics measurement of the  $^{95}\text{Mo}(d, p\gamma)$  surrogate for  $(n, \gamma)$  are presented here. They show that a limited amount of angular momentum, populating at maximum the  $6_1^+$  state in  $^{96}\text{Mo}$ , is brought into the entry state above the neutron separation energy in the  $(d, p)$  reaction. This is similar to what is seen in the preliminary results from the  $^{95}\text{Mo}(n, \gamma)$  measurement at LANSCE, where the  $6_1^+$  state (and no state of higher angular momentum) is populated. The next step is to use the empirical  $\gamma$ -ray emission probabilities from both the normal kinematics  $(d, p\gamma)$  and  $(n, \gamma)$  measurements and calculations of the formation of the compound nucleus as input for calculating  $(n, \gamma)$  cross sections. To realize  $(n, \gamma)$  surrogate reactions of unstable nuclei requires a valid surrogate in inverse kinematics with radioactive ion beams interacting with a deuteron (e.g.,  $\text{CD}_2$ ) target. The GODDESS particle- $\gamma$  spectrometer is poised to complete the surrogate validation efforts with  $^{95}\text{Mo}$  beams and particle-gamma coincidences enabled by the ORRUBA and Gammasphere arrays, respectively.

## Acknowledgements

The authors thank the operations staff at the Texas A&M Cyclotron institute for their exceptional support of the normal kinematics measurement of the  $^{95}\text{Mo}(d, p\gamma)$  reaction. A.R. thanks Giordano Cerizza for useful discussions.

This work is supported in part by the U.S. Department of Energy (DOE) National Nuclear Security Administration (NNSA) Stewardship Science Academic Alliance Programs through Cooperative Agreements No. DE-FG52-08NA28552 and DE-NA0002132 (Rutgers), No. DE-FG52-09NA29467 (TAMU); DOE Contracts DE-AC02-06CH11357 (ANL), No. DE-AC52-07NA27344 (LLNL), No. AC52-06NA25396 (LANL), No. DE-FG52-06 NA26206 (Richmond), DOE Office of Science No. DE-AC05-00OR22725 (ORNL), DE-FG02-96ER40983 (UTK), No. DE-SC0001174 (UTK), DE-FG02-96ER40955 (TTU), No. DE-FG02-05 ER41379 and ), and No. DE-FG02-93ER40773 (TAMU); the National Science Foundation No. 1067906 (Rutgers); and the Department of Energy's NNSA Office of Defense Nuclear Nonproliferation Research & Development (LLNL).

## References

- [1] R. Surman, J. Beun, G.C. McLaughlin, W.R. Hix, Phys. Rev. C **79**, 045809 (2009)
- [2] J.E. Escher, J.T. Burke, F.S. Dietrich, N.D. Scielzo, I.J. Thompson, W. Younes, Rev. Mod. Phys. **84**, 353, (2012)
- [3] V.F. Weisskopf and D.H. Ewing, Phys. Rev. **57**, 472 (1940)
- [4] C. Forssén, F.S. Dietrich, J.E. Escher, R.D. Hoffman, K. Kelley, Phys. Rev. C **75**, 055807 (2007)
- [5] R. Hatarik, L.A. Bernstein, J.A. Cizewski, D.L. Bleuel, J.T. Burke, J.E. Escher, J. Gibelin, B.L. Goldblum, A.M. Hatarik, S.R. Leshner *et al.*, Phys. Rev. C **81**, 011602 (2010)
- [6] J.E. Escher and F.S. Dietrich, Phys. Rev. C **81**, 024612 (2010)
- [7] N.D. Scielzo, J.E. Escher, J.M. Allmond, M.S. Basunia, C.W. Beausang, L.A. Bernstein, D.L. Bleuel, J.T. Burke, R.M. Clark, F.S. Dietrich *et al.*, Phys. Rev. C **81**, 034608 (2010)
- [8] A.R. De L. Musgrove, B.J. Allen, J.W. Boldeman, R.L. Macklin, Nucl. Phys. A **270**, 108 (1976)
- [9] S.R. Leshner, L. Phair, L.A. Bernstein, D.L. Bleuel, J.T. Burke, J.A. Church, P. Fallon, J. Gibelin, N.D. Scielzo, M. Wiedeking, Nucl. Inst. and Meth. in Phys. Sect. A **621**, 286 (2010)
- [10] R.J. Casperson, J.T. Burke, N.D. Scielzo, J.E. Escher, E. McCleskey, M. McCleskey, A. Saastamoinen, A. Spiridon, A. Ratkiewicz, A. Blanc *et al.*, Phys. Rev. C **90** 034601 (2014)
- [11] NIDC Staff, private communication (2012)
- [12] F.S. Goulding, D.A. Landis, J. Cerny, R.H. Pehl, Nucl. Inst. and Meth. **31**, 1 (1964)
- [13] NNDC, <http://www.nndc.bnl.gov/>
- [14] N.D. Scielzo, J.E. Escher, J.M. Allmond, M.S. Basunia, C.W. Beausang, L.A. Bernstein, D.L. Bleuel, J.T. Burke, R.M. Clark, F.S. Dietrich *et al.*, Phys. Rev. C **85**, 054619 (2012)
- [15] W. Verkerke and D. Kirkby <http://roofit.sourceforge.net/>
- [16] J.A. Becker and R.O. Nelson, Nuclear Physics News **7**, 11 (1997)
- [17] I.Y. Lee, Nucl. Phys. A **520**, c641 (1990)
- [18] S.D. Pain, J.A. Cizewski, R. Hatarik, K.L. Jones, J.S. Thomas, D.W. Bardayan, J.C. Blackmon, C. D. Nesaraja, M.S. Smith, R.L. Kozub, M.S. Johnson, Nucl. Inst. and Meth. in Phys. Sect. B **261**, 1122 (2007)
- [19] A. Ratkiewicz, S.D. Pain, J.A. Cizewski, D.W. Bardayan, J.C. Blackmon, K.A. Chipps, S. Hardy, K.L. Jones, R.L. Kozub, C.J. Lister *et al.*, AIP Conference Proceedings **1525**, 487 (2013)
- [20] , A. Ratkiewicz, J.A. Cizewski, S. Hardy, M.E. Howard, B. Manning, C.M. Shand, S.D. Pain, D.W. Bardayan, M. Matos, J.C. Blackmon *et al.*, Fission and Properties of Neutron-Rich Nuclei pp. 326-331 (2012)
- [21] C.N. Davids and J.D. Larson, Lecture Notes in Physics **317**, 313 (1988)
- [22] K.Y. Chae, S. Ahn, D.W. Bardayan, K.A. Chipps, B. Manning, S.D. Pain, W.A. Peters, K.T. Schmitt, M.S. Smith, S.Y. Strauss, Nucl. Inst. and Meth. in Phys. Sect. B **751**, 6 (2014)

